CHEMISTRY
A EUROPEAN JOURNAL

DOI: 10.1002/chem.201000267

Probing Surface Sites of TiO_2: Reactions with $[HRe(CO)_5]$ and $[CH_3Re(CO)_5]$

Rodrigo J. Lobo-Lapidus[a, b] and Bruce C. Gates*[a]

Abstract: Two carbonyl complexes of rhenium, $[HRe(CO)_5]$ and $[CH_3Re(CO)_5]$, were used to probe surface sites of TiO_2 (anatase). These complexes were adsorbed from the gas phase onto anatase powder that had been treated in flowing O_2 or under vacuum to vary the density of surface OH sites. Infrared (IR) spectra demonstrate the variation in the number of sites, including Ti^{+3}–OH and Ti^{+4}–OH. IR and extended X-ray absorption fine structure (EXAFS) spectra show that chemisorption of the rhenium complexes led to their decarbonylation, with formation of surface-bound rhenium tricarbonyls, when $[HRe(CO)_5]$ was adsorbed, or rhenium tetracarbonyls, when $[CH_3Re(CO)_5]$ was adsorbed. These reactions were accompanied by the formation of water and surface carbonates and removal of terminal hydroxyl groups associated with Ti^{+3} and Ti^{+4} ions on the anatase. Data characterizing the samples after adsorption of $[HRe(CO)_5]$ or $[CH_3Re(CO)_5]$ determined a ranking of the reactivity of the surface OH sites, with the Ti^{+3}–OH groups being the more reactive towards the rhenium complexes but the less likely to be dehydroxylated. The two rhenium pentacarbonyl probes provided complementary information, suggesting that the carbonate species originate from carbonyl ligands initially bonded to the rhenium and from hydroxyl groups of the titania surface, with the reaction leading to the formation of water and bridging hydroxyl groups on the titania. The results illustrate the value of using a family of organometallic complexes as probes of oxide surface sites.

Keywords: EXAFS spectroscopy · IR spectroscopy · rhenium carbonyl complexes · surface chemistry · titania

Introduction

The importance of supports in supported metal catalysts is becoming increasingly evident, especially when the metal particles become so small that they are in the nano-size region—because the metal–support interactions are then maximized.[1] Although properties such as the support surface area influence catalyst performance, it is the nature and extent of the interactions between the metal and the support that are crucial to determine the role of the support in catalysis by supported metal nanoclusters.[2]

In the development of this subject, titania as a support has played a central role, because the metal–support interactions have been among the strongest observed—this support even migrates after high-temperature treatments to envelope metal particles on it.[3,4] Much of the recent research on titania has been focused on its photocatalytic properties and its potential for use in catalytic photo-splitting of water and oxidation of organic compounds. Numerous investigations have focused on photo-generation of defect sites[5] and radical species[6,7] on titania surfaces, because they have been implicated in catalysis by titania subjected to UV radiation. Although much of the current understanding of titania surface chemistry has emerged from investigations of clean, dehydroxylated, single-crystal surfaces,[5] this understanding is not always sufficient for some applications (such as catalysis), because, on the industrial scale, the titania is used in the form of high-area hydroxylated powders, which are structurally more complex that the single crystals.

It has been established broadly that the degree of surface hydroxylation of metal oxides such as titania can markedly

[a] R. J. Lobo-Lapidus, B. C. Gates
Chemical Engineering and Materials Science
University of California at Davis
One Shields Ave., Davis, CA 95616 (USA)
Fax: (+1) 530-7521031
E-mail: bcgates@ucdavis.edu

[b] R. J. Lobo-Lapidus
Chemical Sciences and Engineering Division
Argonne National Laboratory
9700 S. Cass Avenue, Argonne, IL 60439 (USA)

Supporting information for this article is available on the WWW under http://dx.doi.org/10.1002/chem.201000267.

affect the nature of the surface sites and their catalytic properties and the properties of the metal sites that are dispersed on the metal oxide.[8] Titania surfaces incorporate various types of hydroxyl groups, differentiated by the type and number of Ti atoms to which they are bonded (e.g., OH groups bonded to Ti^{3+} or Ti^{4+} atoms).[9] An important tool to differentiate these groups and understand their chemistry is infrared (IR) spectroscopy. Characterization of surface OH groups on high-area titania can provide insight into the reactivity of partially reduced surface sites (Ti^{3+}), because the OH groups that are bonded to the surface at these sites are characterized by IR bands with frequencies significantly different from those of OH groups bonded to fully oxidized surface Ti atoms (Ti^{4+}).[9]

Much of the understanding of the reactivity of surfaces has emerged from their characterization with adsorbed probe molecules, which are often interrogated with IR spectroscopy. Characteristics of an adsorbed probe may provide insights into the properties of the surface sites to which they are bonded, such as their acidity and the coordinative unsaturation of the metal atoms.[10]

Typical probe molecules are small, such as H_2, CO,[10] CO_2,[11] NH_3,[12] and organics, including CH_4[13] and pyridine.[12] These probes are characterized by some limitations: 1) they may be noninnocent, changing the surface site by interacting with it,[14] and 2) they fail to provide any information about metal–support interactions.

In contrast to these commonly used probes, organometallic compounds, which are less well explored as surface probes, offer advantages that may overcome some of the limitations of the commonly used probes. For example, organometallic probes may provide direct information about metal–support interactions. Furthermore, the prospect of changing both the metal in the probe and the ligands bonded to it confers flexibility in terms of the reactivity of the probe and its bonding to the support; a subtle tunability may be provided by a family of probes characterized by small variations from one member to another. Moreover, a heavy-metal atom in an organometallic probe enables the use of characterization tools such as transmission electron microscopy and X-ray absorption spectroscopy that are limited in applicability when the probe molecules contain only light atoms.

Families of metal carbonyl complexes are potentially good complementary probes, because the CO vibrations can be easily measured by IR spectroscopy and are sensitive to the environment of the metal to which the CO groups are bonded, determined by the other ligands bonded to the metal, often including the support.[15] Furthermore, when removed from the metal, the CO ligands can form a variety of surface or gas-phase species that are readily characterized and may provide insights into the surface reactivity.

Complexes of the oxophilic metal rhenium are appealing as probes of sites on metal oxides, because rhenium can form strong Re–O bonds with the surface, stronger than the metal–oxygen bonds formed by group 8 metals. Rhenium complexes are also attractive because they are available in a family with the composition $[LRe(CO)_5]$ (where L can be one of several ligands, including H^- and CH_3^-).[16,17]

We now report the use of $[HRe(CO)_5]$ and $[CH_3Re(CO)_5]$ to probe the surfaces of titania (anatase) treated under different conditions to vary the density of the surface sites (Ti^{3+}–OH and Ti^{4+}–OH).[9] We have characterized our titania samples, with and without the probes, by IR spectroscopy to provide information about the hydroxyl groups on the titania and the carbonyl ligands on the rhenium, and to differentiate the various titania surface sites to which the hydroxyl groups might be bonded. We have also interrogated the immediate surroundings of the surface-bound rhenium (including the titania anchoring sites) with extended X-ray absorption fine structure (EXAFS) spectroscopy measured at the rhenium L_{III} edge.

Results

Characterization of titania after various treatments and identification of surface OH groups

Treatments in O_2 and under vacuum: Titania prepared by a sol-gel synthesis was calcined at 723 K in flowing O_2. Then it was treated at various temperatures under vacuum or in flowing O_2, to provide samples containing various densities of surface Ti^{+3} sites.[18] In the following, the titania samples are labeled according to their treatments. When the treatments took place in flowing O_2, the samples are labeled with the subscript "ox" and when the treatment was under vacuum, the samples are labeled with the subscript "vac". These are followed by subscripts denoting the treatment temperature in Kelvin. Thus, for example, $TiO_{2vac673}$ indicates anatase treated under vacuum at 673 K.

IR spectra characterizing $TiO_{2vac723}$ include five main peaks in the 3400–3800 cm^{-1} region (Figure 1 and Table 1),

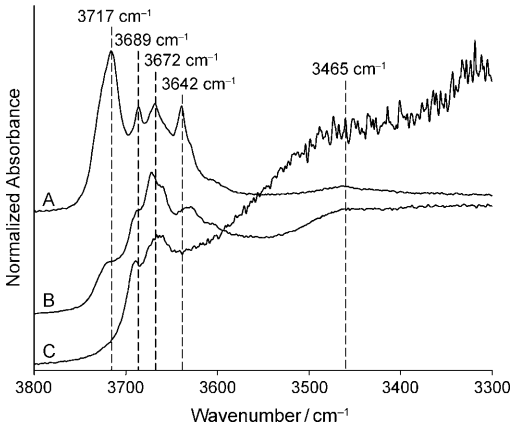

Figure 1. Normalized IR spectra in the ν_{OH} region characterizing titania samples treated under various conditions: A) Under vacuum at 723 K for 4 h, B) in flowing O_2 at 723 K for 4 h, and C) under vacuum at 723 K for 4 h, followed by exposure to air for 5 min. Spectra are normalized so that the peak at $\tilde{\nu}=3672\ cm^{-1}$ has an absorbance of 1.0. The spectra are offset for clarity.

Table 1. IR peaks in the OH-stretching region characterizing titania.

Titania form and phase of sample	Treatment	Scan conditions	Band locations [cm^{-1}]	Assignment	Ref.
titania powder (anatase)	4 h vacuum treatment at 723 K	vacuum	3717 3689 3672 3642		this work
titania powder (anatase)	4 h O_2 treatment at 723 K	vacuum	3717 3689 3672 3642		this work
titania powder	dried in N_2	N_2	3693 3674 3655 3636	Ti^{4+}–OH (on rutile) Ti^{4+}–OH vicinal (on anatase) Ti^{4+}–OH (on rutile) $(Ti^{4+})_2$–OH (on anatase)	[19]
P-25 (a mixture of rutile and anatase)	UV irradiation in vacuum UV irradiation in O_2	vacuum or O_2 O_2	3716 3647 3682 3416	Ti^{3+}–OH Ti^{4+}–OH Ti^{4+}–OH+	[9]

located at $\tilde{\nu}=3717$, 3689, 3672, 3642, and 3465 cm^{-1}. Table 1 shows the peak positions characterizing the groups on the titania samples, along with literature assignments. The literature reports were used as a basis for assigning these IR bands; the bands listed in the preceding sentence are assigned respectively to OH groups that are part of Ti^{3+}–OH, Ti^{4+}–OH, Ti^{4+}–OH, and $(Ti^{4+})_2$–OH species and to OH groups in adsorbed water.[9,18–20] Although bands at $\tilde{\nu}=3689$ and 3672 cm^{-1} have both been assigned to Ti^{4+}–OH groups,[9,19] it is clear from the spectra that each corresponds to separate modes, suggesting that the coordination of the Ti atoms to OH is different, corresponding to the different frequencies.[21] We lack sufficient information to determine the differences between these two sites.

Exposure of $TiO_{2vac723}$ to moisture-containing air resulted in the complete disappearance of the band at $\tilde{\nu}=3717$ cm^{-1} and an increase in the intensity of the band associated with adsorbed water (Figure 1C). Smaller changes in the bands at $\tilde{\nu}=3672$ and 3642 cm^{-1} were also observed.

IR spectra characterizing the sample treated in flowing O_2 (TiO_{2ox723}, Figure 1B) indicate the presence of the same OH bands observed in the spectra of $TiO_{2vac723}$; however, consistent with previous observations, the intensity of the band at $\tilde{\nu}=3717$ cm^{-1} relative to that of the Ti^{+4}–OH bands was significantly reduced,[18,20] which is in line with the assignment of the band at $\tilde{\nu}=3717$ cm^{-1} to Ti^{+3}–OH groups that we would expect to have been almost completely removed by the treatment in O_2.[9,22] In summary, the assignment of the band at $\tilde{\nu}=3717$ cm^{-1} to Ti^{+3}–OH is based on the intensity changes after treatments of the titania in O_2 or under vacuum and its position in the IR spectra.

Effects of treatment temperature on density of surface Ti^{3+}–OH and Ti^{4+}–OH sites: The normalized IR spectra characterizing titania samples treated under vacuum at various temperatures (Figure 2) show that the intensity of the peak assigned to OH groups on Ti^{3+} sites increased monotonically with increasing temperature, relative to the peaks characterizing Ti^{+4}–OH. Thus, the number of Ti^{3+}–OH sites relative to the total number of OH sites was greater at higher temperatures. Because these spectra are normalized, the results suggest that either the number of Ti^{3+} sites increased with increasing treatment temperature, or that the number of OH groups bonded to Ti^{4+} sites decreased, or a combination of the two effects. To resolve this issue, it was helpful to titrate the various surface sites on the support, as described below.

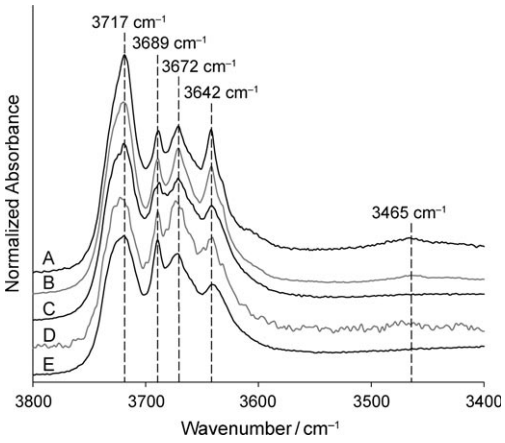

Figure 2. Normalized IR spectra in the ν_{OH} region characterizing titania samples treated under vacuum for 4 h at various temperatures: A) 723, B) 673, C) 623, D) 573, and C) 523 K. Spectra are normalized so that the peak at $\tilde{\nu}=3672$ cm^{-1} has a height of 1.0. The spectra are offset for clarity.

Adsorption of $[HRe(CO)_5]$ on titania

To form titania-supported rhenium species, the complexes $[HRe(CO)_5]$ and, separately, $[CH_3Re(CO)_5]$ were brought in contact with the titania powder through the gas phase, as the powder was stirred. The resulting samples were evacuated and subjected to characterization (all procedures were

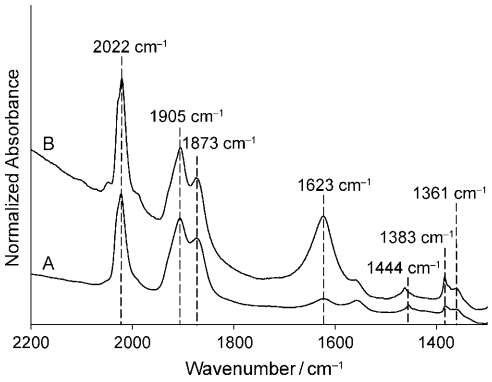

Figure 3. Normalized IR spectra in the $\tilde{\nu}=2200$–$1300\ cm^{-1}$ region characterizing titania samples that were first exposed to $[HRe(CO)_5]$ vapor and then evacuated: A) $TiO_{2vac723}$ and B) TiO_{2ox723}. Spectra are normalized so that the height of the peak at $\tilde{\nu}=1905\ cm^{-1}$ is equal to 1.0. The spectra are offset for clarity.

performed with exclusion of air and moisture; see the Experimental Section).

IR spectra demonstrate adsorption and decarbonylation of [HRe(CO)$_5$] on titania: IR data characterizing the samples $TiO_{2vac723}$ and TiO_{2ox723}, after exposure to $[HRe(CO)_5]$ (Figure 3), show that, after adsorption, each sample incorporated carbonyl species and each was characterized by three major peaks, at $\tilde{\nu}=2022$, 1905, and 1873 cm^{-1}. These peaks indicate the presence of metal carbonyls.[15]

The IR spectra of rhenium pentacarbonyls in solution often only show three CO bands (as a consequence of the symmetry of the molecule and/or of the weak absorption of some of the vibrational modes).[23,24] When $[HRe(CO)_5]$ is adsorbed on MgO it forms species identified as rhenium pentacarbonyls that are characterized by only two (broad) ν_{CO} bands in the IR spectrum.[25] The ν_{CO} peaks characterizing such species are typically in a frequency range of about $\tilde{\nu}=1970$–$2150\ cm^{-1}$ (Table 2).[26–28]

Thus, the presence of peaks at $\tilde{\nu}=1905$ and $1873\ cm^{-1}$ in the spectrum of our $TiO_{2vac723}$ sample after exposure to $[HRe(CO)_5]$ is strong evidence that the surface species formed are not rhenium pentacarbonyls. Moreover, the positions and relative intensities of these peaks are in excellent agreement with those characterizing rhenium tricarbonyls on MgO (formed by treatment of the species formed on the TiO_2 surface by adsorption of $[HRe(CO)_5]$ or $[H_3Re_3(CO)_{12}]$),[25] on other supports,[29,30] and in solution[31,32] (Table 2). Thus, we infer that our titania-supported species formed from $[HRe(CO)_5]$ were rhenium tricarbonyls. Furthermore, the strong intensity of each of the three peaks in each of the spectra suggests that the rhenium tricarbonyls were likely characterized by C_s symmetry.[32]

However, because IR spectroscopy is typically not sufficient to identify specific metal carbonyl species or to determine whether they are bonded to the support, we have obtained complementary information by EXAFS spectroscopy.

EXAFS data demonstrate chemisorption of [HRe(CO)$_5$] on $TiO_{2vac723}$: Analysis of the EXAFS data characterizing $TiO_{2vac723}$ after exposure to $[HRe(CO)_5]$ led to two structural models that fit the data well (Table 3) and include physically appropriate fit parameters. Plots for each of the models are presented in the Supporting Information.

The first of these models (Table 3, model 1) includes a Re–C contribution at 1.99 Å and a multiple-scattering Re–O contribution at 3.13 Å, with coordination numbers of 5.4 and 5.7, respectively, which match each other within error. The data also show the presence of Re–O contributions at 2.22 Å and 2.50 Å.

The second model (Table 3, model 2) also includes a Re–C contribution and a multiple-scattering Re–O contribution, at distances similar to those observed for model 1 (1.82 and 3.09 Å, respectively). However, in model 2 the corresponding coordination numbers are 2.8 and 3.4, which match each other within error but are significantly different from those calculated for model 1. Two Re–O contributions are also observed for model 2, at 1.92 and 3.29 Å.

Each of the models is characterized by a Re–C contribution and a multiple-scattering Re−O contribution, characteristic of carbonyl ligands attached to the rhenium; these Re–

Table 2. IR peaks in the ν_{CO} stretching region characterizing titania exposed to $[HRe(CO)_5]$ or $[CH_3Re(CO)_5]$ and of reference compounds.

Metal carbonyl species	Solvent or support	Peak positions [cm^{-1}]	Ref.
sample formed from $[HRe(CO)_5]$ on $TiO_{2vac723}$	titania	2022, 1905, 1873	this work
sample formed from $[CH_3Re(CO)_5]$ on $TiO_{2vac723}$[a]	titania	2102, 1999, 1986, 1959, 1912	this work
sample formed from $[CH_3Re(CO)_5]$ on TiO_{2ox723}	titania	2100, 2026, 1996, 1958, 1912, 1875	this work
$[Re(CO)_3\{O-Al\}\{HO-Al\}_2]$[a]	Al_2O_3	2028,1915, 1887	[29]
$[Re(CO)_3\{O-Mg\}\{HO-Mg\}_2]$[a]	MgO	2028, 1905, 1862	[29]
$[Re(CO)_3\{O^{2-}\}_2\{O^{2-}\}]$	zeolite Y	2133, 2056, 2036, 2021, 1984, 1944	[53]
[Re(CO)$_3$(2,2-bpy)(py)][b]	AlMCM-41	2045,[f] 1940,[f] 1925[f]	[30]
[Re(CO)$_4$O*i*Pr]I[c]	benzene	2105, 2022, 2001, 1964, 1960	[30]
$[Re(CO)_4\{PL_3\}]I$[d]	benzene	2111–2099, 2030–2007, 2001–2008, 1968–1945, 1960–1951[g]	[42]
[L′Re(CO)$_5$][e]	CCl_4	2148–2143, 2075–2065, 2040–2029, 2014–1998	[26]
$[C_nH_{2n+1}Re(CO)_5]$ ($n=1$–12)	hexane	2131–2129, 2060–2058, 2026–2014, 1999–1998	[27]
$[XRe(CO)_5]$ (X = Cl, Br, I)	–	2156–2145, 2082–2076, 2045–2042, 1987–1982	[28]

[a] The brackets represent surface groups. [b] Bpy = bipyridine, py = pyridine. [c] O*i*Pr = isopropoxide. [d] L = CH_3, phenyl, O-*o*-toluene, OCH_3, OC_2H_5. [e] L′ = one of many fluorinated ligands (e.g., $C_3F_7^-$, $C_2F_3^-$, C_5F_4N, or $CF_3CH{=}CH^-$). [f] Values estimated from graphical data in reference [30]. [g] Peak not present in spectra of all complexes.

Table 3. EXAFS fit parameters for the best fir model characterizing samples prepared from $[HRe(CO)_5]$ and $TiO_{2vac723}$.[a]

Absorber–backscatterer pair	N[b]	R [Å][b]	$10^3\times\Delta\sigma^2$ [Å^2][b]	ΔE_0 [eV][b]	$(\Delta\chi)^2$[c]
model 1					
Re–C	5.4±1.3	1.99±0.04	7.5±1.8	−9.1±1.7	49.5
Re–O	1.1±0.4	2.50±0.05	1.8±2.2	0.0±0.5	
Re–O (MS)[d]	5.7±1.2	3.13±0.04	3.2±0.9	−0.4±0.0	
Re–O	1.1±0.5	2.22±0.04	0.4±1.3	0.0±0.5	
model 2					
Re–C	2.8±0.6	1.82±0.04	3.3±1.1	−9.4±1.6	47.5
Re-O	2.5±0.5	1.92±0.04	0.4±0.4	0.1±0.2	
Re–O (MS)[d]	3.4±0.8	3.09±0.04	1.8±1.1	−9.4±1.6	
Re–O	5.7±1.3	3.29±0.04	1.8±0.9	0.1±0.2	

[a] k range: 2.58–12.09 Å^{-1}, R range: 1.00–3.50 Å, error in data determined by Fourier filtering: 0.0019. Maximum number of justifiable fit parameters determined by the Nyquist theorem is 17. [b] The error bounds correspond to the total error in the parameter estimate, including precision and accuracy. The estimated accuracies are as follows: $N=\pm20\%$, $R=\pm0.04$ Å, $\Delta\sigma^2=\pm20\%$, $\Delta E_0=\pm20\%$; N, coordination number, R, absorber–backscatter distance, $\Delta\sigma^2$, Debye–Weller factor. [c] $(\Delta\chi)^2$ is a measure of the quality of the fit, as defined in reference [33]. [d] Multiple-scattering contribution incorporating linear Re-C-O moiety.

Table 4. EXAFS fit parameters for models characterizing samples prepared from $[HRe(CO)_5]$ and TiO_{2ox723}.[a]

Absorber–backscatterer pair	N[b]	R [Å][b]	$10^3\times\Delta\sigma^2$ [Å^2][b]	ΔE_0 [eV][b]	$(\Delta\chi)^2$[c]
model 3					
Re–C	5.0±1.2	1.98±0.05	1.2±0.9	−8.2±1.2	49.5
Re–O	1.7±0.5	2.41±0.06	1.8±1.9	−1.0±1.8	
Re–O (MS)[d]	5.4±1.1	3.12±0.04	2.7±0.8	−0.1±0.2	
Re–O	2.2±0.7	2.14±0.05	0.4±1.4	−1.0±1.8	
model 4					
Re–C	2.8±0.6	1.79±0.06	6.0±2.4	−9.7±1.0	29.5
Re–O	3.2±0.7	1.87±0.05	1.0±0.8	7.9±2.2	
Re–O (MS)[d]	3.6±1.0	3.08±0.05	4.5±3.6	−9.7±1.0	
Re–O	4.7±1.4	3.18±0.05	0.5±1.7	7.9±2.2	

[a] k range: 2.63–12.00 Å^{-1}, R range: 1.00–3.50 Å, error in data determined by Fourier filtering: 0.0033. Maximum number of justifiable fit parameters determined by the Nyquist theorem is 16. [b] The error bounds correspond to the total error in the parameter estimate, including precision and accuracy. The estimated accuracies are as follows: : $N=\pm20\%$, $R=\pm0.04$ Å, $\Delta\sigma^2=\pm20\%$, $\Delta E_0=\pm20\%$. [c] $(\Delta\chi)^2$ is a measure of the quality of the fit, as defined in reference [33]. [d] Multiple-scattering contribution incorporating Re-C-O atom arrangement.

CO coordination numbers in model 2 (roughly three) indicate that the species formed upon adsorption were, on average, rhenium tricarbonyls, consistent with the IR results and indicating that the adsorption of $[HRe(CO)_5]$ on $TiO_{2vac723}$ led to decarbonylation of the rhenium complex. The agreement between model 2 and the IR data suggests that this model better approximates the rhenium species on the TiO_2 surface than model 1. Furthermore, although both models led to satisfactory fits with physically appropriate parameters, the value of $(\Delta\chi)^2$[33] (Table 3) indicates that the data are better approximated by model 2 than model 1, which bolsters our selection of model 2.

The distance of the shortest Re–O contribution in model 2 (1.92 Å) is in good agreement with similar contributions characterizing rhenium complexes bonded to other metal oxides, in which the oxygen atom is part of the support surface.[25,34,35] Thus, this result suggest that each rhenium carbonyl species was bonded to the titania surface; also, the Re–O coordination number of 2.5 (with an uncertainty of about ±20%) indicates that it was bonded through approximately three Re−O bonds. The distance characterizing the other Re–O contribution (3.29 Å) indicates that the oxygen atoms in that contribution were not bonded to the Re atoms, consistent with the inference that the average number of Re−O bonds was approximately three.

EXAFS data demonstrate chemisorption of $[HRe(CO)_5]$ on TiO_{2ox723}: As for the sample mentioned previously, fitting of the EXAFS data led to two models (Table 4) that approximate the data well and include physically appropriate parameters (plots for each of the models are given in the Supporting Information).

Each model incorporates a Re–C contribution (at a distance of 1.98 Å for model 3 and 1.79 Å for model 4) and a multiple-scattering Re–O contribution (at 3.12 Å for model 3 and at 3.08 Å for model 4), with Re–C and multiple-scattering Re–O coordination numbers that match each other within error; the value is approximately five for model 3 and approximately three for model 4 (Table 4). Each of these models also includes a short Re–O contribution, at 2.14 Å for model 3 and 1.87 Å for model 4, and a Re–O contribution at a longer distance—the distances are markedly different for the two models (2.41 Å for model 3 and 3.18 Å for model 4).

Each of the two models led to a good fit of the data with physically appropriate parameters. The value of $(\Delta\chi)^2$ indicates that model 4 provides the better representation of the data, thus, model 4 is preferred.

The corresponding coordination numbers characterizing the Re–C (2.8) and multiple-scattering Re–O contributions (3.6) indicate the presence of rhenium tricarbonyls, and this result implies that $[HRe(CO)_5]$ was decarbonylated upon adsorption on TiO_{2ox723}, a result similar to that determined for the sample formed from $[HRe(CO)_5]$ and $TiO_{2vac723}$. The IR data are in good agreement with this result and thus, further validate the selection of model 4. The Re–O contribution at 1.87 Å with a coordination number of 3.2 suggests that each Re atom was bonded to approximately three oxygen atoms of the titania surface. The result essentially matches that characterizing the sample formed from $[HRe(CO)_5]$ and $TiO_{2vac723}$.

Formation of water and carbonates as a result of adsorption/decarbonylation of $[HRe(CO)_5]$: When $[HRe(CO)_5]$ was adsorbed on $TiO_{2vac723}$ and on TiO_{2ox723}, several bands appeared in the 1700–1300 cm^{-1} region of the IR spectra (Figure 3). Table 5 provides a summary of these bands and shows, for

Table 5. IR peaks in the $\tilde{\nu}=1700$–$1300\ cm^{-1}$ region characterizing the samples of titania and other metal oxides after various treatments.

Sample	Treatment	Scan conditions	Band locations [cm^{-1}]	Assignment	Ref.
sample formed from $[HRe(CO)_5]$ on titania	none	vacuum	1383, 1453 1362, 1443, 1623 1557	monodentate carbonate bicarbonates, CO_2^-, etc.	this work
sample formed from $[CH_3Re(CO)_5]$ on titania	none	vacuum	1382, 1453 1349, 1407, 1619 1508	monodentate carbonate bicarbonate	this work
titania	CO_2 adsorption	–	1319, 1579 1376, 1462 1445 1532 1725	bidentate carbonate monodentate carbonate free carbonate bridging carbonate	[36]
titania (anatase)	CO_2 adsorption	vacuum	1320, 1580 1500	CO_2^- carbonate-like	[37]
MCO_3[a]	–	mulls or dry powder	1410–1450	carbonates	[40]
$M'CO_3H$[b]	–	mulls or dry powder	1370–1300 1400–1410 1620–1630	bicarbonates	[40]
magnesia	calcination at 673 K	in flowing CO_2	1340, 1520 1385, 1500 1413, 1540 1375, 1668 1645, 1400	monodentate carbonate monodentate carbonate monodentate carbonate bicarbonates bidentate carbonates	[38]
titania powder[c]	dried in N_2	N_2	1511, 1391 1421	monodentate carbonate noncoordinated carbonate	[19]

[a] Range shown for bands present in all carbonates that are discussed in ref. [30]. M = Li_2, Na_2, K_2, Mg, Ca, Ba, Co, or Pb. [b] Range shown for bands present in all bicarbonates that are discussed in this article. M′ = NH_4, K, or Na. [c] Inferred from IR to contain rutile and anatase phases.

comparison, the positions of IR bands characterizing different metal oxides after various treatments. On the basis of a comparison with the values reported in these references, we assign the band at approximately $\tilde{\nu}=1623\ cm^{-1}$ characterizing our samples made from $[HRe(CO)_5]$ and either $TiO_{2vac723}$ or TiO_{2ox723} to water adsorbed on titania. This result indicates that water is formed as a result of the adsorption of $[HRe(CO)_5]$; we suggest that it resulted from the reaction of $[HRe(CO)_5]$ with surface-bonded hydroxyl groups of titania.

Adsorption of $[HRe(CO)_5]$ also led to the appearance of peaks at $\tilde{\nu}=1382$ and $1453\ cm^{-1}$, which are associated with monodentate carbonates on titania (Table 5).[36,37] We infer that the presence of formates and other species that contain C–H bonds is unlikely, because no bands were observed in the 3200–2800 cm^{-1} region characteristic of C–H stretching vibrations.

The presence of additional bands in the 1700–1300 cm^{-1} region indicates that other species were formed as well, but we lack sufficient information to assign them unambiguously; however, on the basis of their positions, we suggest that they might indicate carbonates and/or bicarbonates.[36–40]

Removal of Ti^{3+}–OH sites and formation of water on titania as a result of adsorption of $[HRe(CO)_5]$: The OH stretching region of the IR spectra characterizing $TiO_{2vac723}$ after exposure to $[HRe(CO)_5]$ (Figure 4) includes no evidence of Ti^{3+}–OH bands ($\tilde{\nu}=3717\ cm^{-1}$), indicating that the Ti^{3+}–OH sites were removed during the adsorption of the rhenium carbonyl complex. This behavior suggests a removal of Ti^{3+}–OH sites from anatase parallel to that reported for the reaction with $[H_3Re_3(CO)_{12}]$,[18] which presumably resulted

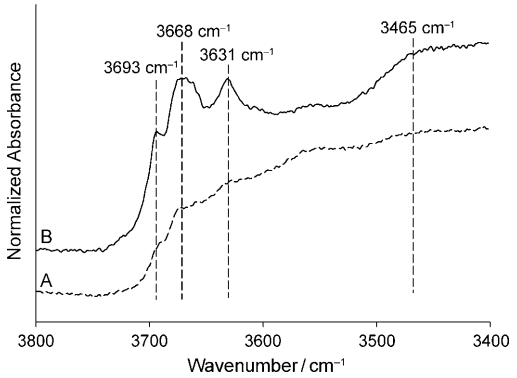

Figure 4. Normalized IR spectra in the 3800–3400 cm^{-1} region characterizing titania samples exposed to $HRe(CO)_5$ vapor and then evacuated. (A) $TiO_{2vac723}$, (B) TiO_{2ox723}. Spectra are normalized so that the peak at 3672 cm^{-1} has a height of 1.0. The spectra are offset for clarity.

from deprotonation of the $[H_3Re_3(CO)_{12}]$; however, in that case there was no evidence of decarbonylation of the rhenium species, in contrast to the decarbonylation of $[HRe(CO)_5]$ reported here.

Simultaneously with the decrease in intensity of the band at $\tilde{\nu}=3717\ cm^{-1}$ when $[HRe(CO)_5]$ was adsorbed, the very broad feature at approximately $\tilde{\nu}=3465\ cm^{-1}$, associated with adsorbed water, grew significantly as a result of adsorption of $[HRe(CO)_5]$. This result is in agreement with the appearance of the band at $\tilde{\nu}=1623\ cm^{-1}$, which is also associated with water adsorbed on titania.

To better understand the conversion of OH sites, IR spectra characterizing $TiO_{2vac723}$ were recorded while $[HRe(CO)_5]$ passed over the sample in a stream of helium (Figures 5 and 6). During the initial part of the experiment (when the $[HRe(CO)_5]$ was at 196 K), the rhenium carbonyl adsorbed slowly on the titania, as shown by a slow increase in the intensities of the bands in the ν_{CO} region, $\tilde{\nu}=2200$–$1800\ cm^{-1}$ (Figure 5). Concomitant with this increase, the bands associated with Ti^{4+}–OH groups and adsorbed water (at $\tilde{\nu}=3642$ and $3465\ cm^{-1}$, respectively) slowly increased.

During the second part of the experiment (with the $[HRe(CO)_5]$ at room temperature), the spectra (Figure 6) show that the intensities of the carbonyl bands increased rapidly (until the absorbance of any such band was so high that the peak was truncated). Concomitantly, the band characteristic of the Ti^{3+}–OH groups (at $\tilde{\nu}=3717\ cm^{-1}$) began to disappear, as did the Ti^{4+}–OH band at $\tilde{\nu}=3689\ cm^{-1}$, suggesting that only terminal hydroxyl groups were removed during the adsorption process. Simultaneously, the band assigned to $(Ti^{4+})_2$–OH (at $\tilde{\nu}=3642\ cm^{-1}$) grew in as the bands in the CO stretching region increased in intensity.

The spectra recorded during this part of the experiment are characterized by an isosbestic point at approximately $\tilde{\nu}=3665\ cm^{-1}$, which is clearly evident in the difference spectra (Figure 6B).

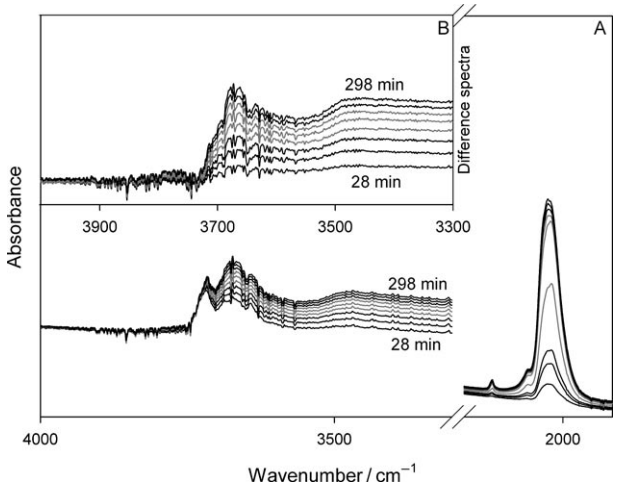

Figure 5. Non-normalized IR spectra characterizing $TiO_{2vac723}$ during adsorption of $[HRe(CO)_5]$, while the $[HRe(CO)_5]$ was held in a cold bath at 196 K. A) Raw spectra recorded at various times during $[HRe(CO)_5]$ adsorption and B) difference spectra: spectra in A) minus spectra of sample before helium flow.

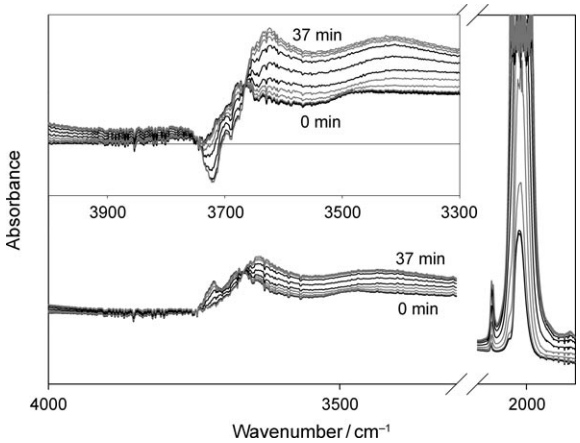

Figure 6. Non-normalized IR spectra characterizing $TiO_{2vac723}$ during adsorption of $[HRe(CO)_5]$, while the $[HRe(CO)_5]$ was warmed up from 196 K to 298 K. A) Raw spectra recorded at various times during $[HRe(CO)_5]$ adsorption and B) difference spectra: spectra in A) minus spectra of sample before helium flow.

Adsorption of $[CH_3Re(CO)_5]$ on titania

IR spectroscopic evidence of decarbonylation and the presence of several species on titania: Various amounts of $[CH_3Re(CO)_5]$ were adsorbed on samples of $TiO_{2vac723}$, corresponding to loadings of 0.4, 1.0, and 1.5 wt% Re. IR spectra characterizing the resulting samples (Figure 7) show that this process led to the formation of surface carbonyl species, with peaks at $\tilde{\nu}=2102$, 1999, 1986, 1959, and $1912\ cm^{-1}$. These bands are the only ones present in the 2200–$1800\ cm^{-1}$ region representing the samples containing 0.4 and 1.0 wt% Re. The Spectrum of the sample containing the highest rhenium loading (1.5 wt% Re) includes additional bands, at $\tilde{\nu}=2026$ and $1875\ cm^{-1}$ (Figure 7). As these bands do not appear in the spectra characterizing the

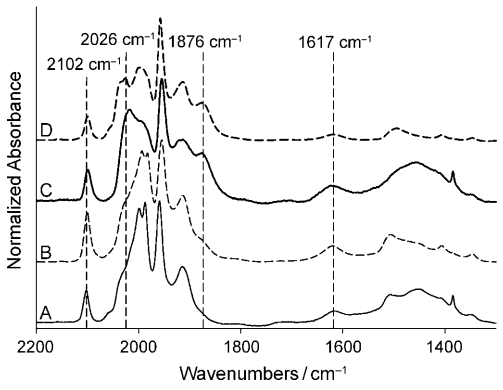

Figure 7. Normalized IR spectra of the $\tilde{\nu}=2200$–$1300\ cm^{-1}$ region characterizing titania samples after adsorption of various amounts of $[CH_3Re(CO)_5]$: A) 0.4, B) 1.0, C) 1.5 wt% Re on $TiO_{2vac723}$, and D) 1.0 wt% Re on TiO_{2ox723}. Spectra are normalized so that the IR peak at $\tilde{\nu}=3673\ cm^{-1}$ is characterized by an absorbance of 1.0. The spectra are offset for clarity.

sample with the lowest loading (0.4 wt% Re), and appear only as weak shoulders in the spectra of the sample containing 1.0% Re, we infer that the species responsible for these bands was present only at higher rhenium loadings. It follows that the samples with these higher loadings are less uniform than those with low loadings.

The band at $\tilde{\nu}\approx2102\ cm^{-1}$, present in the spectra of each of the samples formed from $CH_3Re(CO)_5$, is characterized by a significantly higher frequency than any of those observed for $[HRe(CO)_5]$ in solution,[41] or for the species formed from $[HRe(CO)_5]$ adsorbed on MgO (inferred to be deprotonated rhenium pentacarbonyl),[25] or for $[CH_3Re(CO)_5]$ in solution,[17] or for rhenium tricarbonyls.[25,29,31] Peaks at frequencies similar to those observed with our samples have been observed for rhenium tetracarbonyls in solution,[42] a result that suggests that similar species formed on our samples.

To determine the effect of treatment temperature on the properties of the titania, $[CH_3Re(CO)_5]$ was also adsorbed on $TiO_{2vac573}$, resulting in a sample with a 1.0 wt% Re loading. The IR spectra characterizing the sample in the 1700–2200 cm^{-1} region (see the Supporting Information) include the same peaks observed for the sample containing 0.4 wt% Re on $TiO_{2vac723}$. The relative intensities of these bands are somewhat different for these two samples, but the additional bands that were observed at $\tilde{\nu}=2026$ and 1875 cm^{-1} in the spectra characterizing $TiO_{2vac723}$ incorporating 1.5 wt% Re are not present in the spectra characterizing $TiO_{2vac573}$ incorporating 1.0 wt% Re. This comparison suggests that the species responsible for these bands were not formed in the sample prepared from $TiO_{2vac573}$, notwithstanding the high rhenium loading in the sample.

The IR spectrum characterizing TiO_{2ox723} after exposure to $[CH_3Re(CO)_5]$ in an amount that led to a loading of 1.0 wt% Re (Figure 7D) includes the same five peaks observed in the spectrum characterizing the $TiO_{2vac723}$ sample containing 1.5 wt% Re—including the peaks at $\tilde{\nu}=2026$ and 1875 cm^{-1}, observed only at the higher rhenium loadings in the spectra of $TiO_{2vac723}$. This comparison suggests that the species responsible for these peaks in the sample prepared from TiO_{2ox723} and containing 1.0 wt% Re were also present in the sample containing 1.5 wt% Re—and were not present in the samples containing only 0.4 and 1.0 wt% Re prepared from $TiO_{2vac723}$.

IR spectra showing titration of OH sites by $[CH_3Re(CO)_5]$: The IR spectra of the three samples differ significantly from each other in the $\tilde{\nu}=3200$–3800 cm^{-1} (Figure 8). The spectra characterizing the sample containing the highest loading of rhenium show no evidence of bands at $\tilde{\nu}=3717$ and 3689 cm^{-1}, which are characteristic of Ti^{3+}–OH and Ti^{4+}–OH species, respectively, which were present on the titania before the adsorption. Furthermore, the only peak clearly present in the 3200–3800 cm^{-1} region of the spectrum characterizing the sample containing 1.5 wt% Re is at $\tilde{\nu}=$ 3465 cm^{-1}. This result is contrasted with that obtained for the sample containing 1.0 wt% Re, for which the bands assigned to Ti^{4+}–OH species were still present along with a small shoulder at $\tilde{\nu}\approx3700\ cm^{-1}$ (likely evidence of residual amounts of Ti^{3+} species). Moreover, the spectra of the sample with the lowest Re loading (0.4 wt% Re) include all the peaks present in the spectrum of titania before adsorption of $[CH_3Re(CO)_5]$; however, the relative intensity of the band at $\tilde{\nu}=3717\ cm^{-1}$ was significantly decreased relative to that characterizing the spectrum of the sample before adsorption, a comparison that suggests that some of Ti^{3+} sites were consumed during the adsorption of $[CH_3Re(CO)_5]$. This decrease in intensity of the peak associated with Ti^{3+}–OH groups was tracked by an increase in the broad band at $\tilde{\nu}=3460\ cm^{-1}$ (Figure 8), similar to what was observed during the adsorption of $[HRe(CO)_5]$.

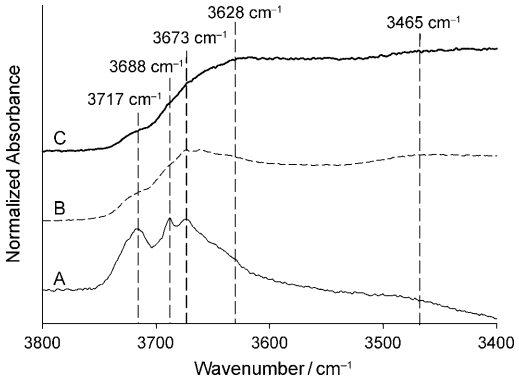

Figure 8. Normalized IR spectra showing the ν_{OH} region that characterizes titania samples after adsorption of various amounts of $[CH_3Re(CO)_5]$: A) 0.4, B) 1.0, and C) 1.5 wt% Re on $TiO_{2vac723}$. Spectra are normalized so that the IR peak at $\tilde{\nu}=3673\ cm^{-1}$ has an absorbance of 1.0. The spectra are offset for clarity.

EXAFS data demonstrate chemisorption of $[CH_3Re(CO)_5]$ on titania still containing Ti^{3+}–OH groups: EXAFS data characterizing the sample containing 1.0 wt% Re on $TiO_{2vac573}$ (Table 6, Figure 9) indicate the presence of a Re–C and a multiple-scattering Re–O contribution, at 1.90 and

Table 6. EXAFS fit parameters for a model characterizing sample prepared from $[CH_3Re(CO)_5]$ and $TiO_{2vac573}$ (1.0 wt% Re loading).[a]

Absorber–backscatterer pair	N[b]	R [Å][b]	$10^3\times\Delta\sigma^2$ [Å^2][b]	ΔE_0 [eV][b]	$(\Delta\chi)^2$[c]
Re–C	3.5±0.8	1.90±0.05	7.7±2.2	−6.0±0.7	54.7
Re–O (MS)[d]	3.8±0.8	3.10±0.04	3.1±0.9	1.3±0.5	
Re–O	3.1±0.8	2.14±0.05	9.8±3.0	−2.2±0.2	
Re–Ti	2.3±0.6	2.53±0.05	8.2±2.9	−2.2±0.2	

[a] k range: 2.70–13.7 Å^{-1}, R range: 1.00–3.50 Å, error in data determined by Fourier filtering: 0.0023. Maximum number of justifiable fit parameters determined by the Nyquist theorem is 16. [b] The error bounds correspond to the total error in the parameter estimate, including precision and accuracy; the estimated accuracies are as follows: $N=\pm20\%$, $R=\pm0.04$ Å, $\Delta\sigma^2=\pm20\%$, $\Delta E_0=\pm20\%$. [c] $(\Delta\chi)^2$ is a measure of the quality of the fit, as defined in reference [33]. [d] Multiple-scattering contribution incorporating Re-C-O atom arrangement.

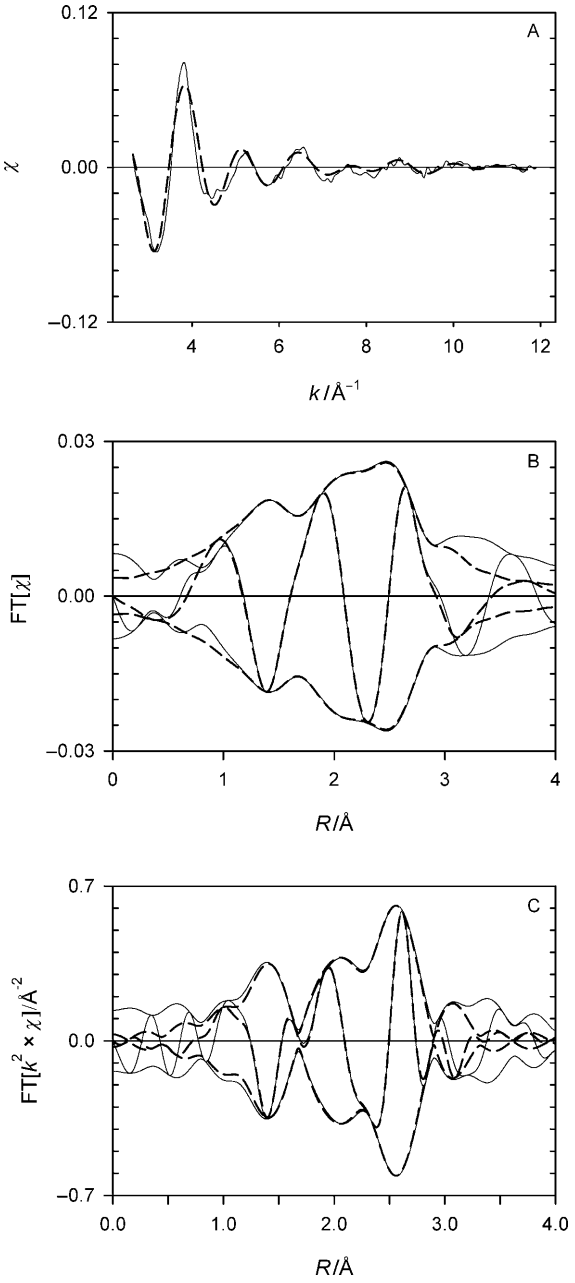

Figure 9. EXAFS data characterizing rhenium carbonyl complexes formed from $TiO_{2vac573}$ and $[CH_3Re(CO)_5]$, (——: data, -----: best-fit model): A) k^1-weighted EXAFS function in k space, B) imaginary part and magnitude of k^1-weighted EXAFS function in R space, and C) imaginary part and magnitude of k^3-weighted EXAFS function in R space.

3.10 Å, respectively, characteristic of carbonyl ligands coordinated to the Re atoms. The coordination numbers of these contributions are 3.5 and 3.8, respectively, suggesting that $[CH_3Re(CO)_5]$ was decarbonylated as a result of the adsorption. The larger coordination numbers, relative to those in samples formed from $[HRe(CO)_5]$, are consistent with the inference that at least some of the species present on the surface were rhenium tetracarbonyls (possibly present with rhenium tricarbonyls).

The data also include a Re–O contribution at a typical bonding distance of 2.14 Å, with a coordination number of 3.1. The distance is significantly longer than that observed for the samples prepared from $[HRe(CO)_5]$, and the comparison suggests that the interaction of the species formed from $[CH_3Re(CO)_5]$ with the support was significantly weaker than those observed for the samples formed from $[HRe(CO)_5]$, and consistent with a lower degree of decarbonylation.

EXAFS data demonstrate chemisorption of $[CH_3Re(CO)_5]$ on titania not containing Ti^{3+}–OH groups: The sample resulting from loading 1.5 wt% Re on $TiO_{2vac723}$ is characterized by a Re–C contribution at 1.93 Å and a multiple-scattering Re–O contribution at 3.08 Å, with coordination numbers of 4.1 and 4.2, respectively (Table 7). These values are

Table 7. EXAFS fit parameters for a model characterizing a sample prepared from $[CH_3Re(CO)_5]$ and $TiO_{2vac723}$ (1.5 wt% Re loading).[a]

Absorber–backscatterer pair	N[b]	R [Å][b]	$10^{-3}\times\Delta\sigma^2$ [Å^2][c]	ΔE_0 [eV][b]	$(\Delta\chi)^2$[c]
Re–C	4.1±1.1	1.93±0.05	7.7±2.6	−8.4±1.0	20.1
Re–O (MS)[d]	4.2±0.9	3.08±0.05	4.5±1.4	2.3±0.8	
Re–O	3.1±1.0	2.14±0.05	5.0±2.3	−3.9±0.1	
Re–O	2.9±0.9	2.46±0.05	10.9±4.1	−3.9±0.1	

[a] k range: 2.59–11.92 Å^{-1}, R range: 1.00–3.50 Å, error in data determined by Fourier filtering: 0.0033. Maximum number of justifiable fit parameters determined by the Nyquist theorem is 16. [b] The error bounds correspond to the total error in the parameter estimate, including precision and accuracy; the estimated accuracies are as follows: N $N=\pm20\%$, $R=\pm0.04$ Å, $\Delta\sigma^2=\pm20\%$, $\Delta E_0=\pm20\%$. [c] $(\Delta\chi)^2$ is a measure of the quality of the fit, as defined in reference [33]. [d] Multiple-scattering contribution incorporating Re-C-O atom arrangement.

consistent with Re atoms surrounded by approximately four carbonyl ligands each, on average. These coordination numbers are, within error, indistinguishable from those of the sample mentioned in the preceding section. However, because EXAFS spectroscopy is an averaging technique, this result does not rule out the presence of a mixture of species in the sample with the higher rhenium loading (as was indicated by IR spectroscopy).

The sample is also characterized by the presence of Re–O contributions, at 2.14 and at 2.46 Å, with coordination numbers of 3.1 and 2.9, respectively. As before, the former contribution is at a distance indicative of bonding of rhenium to oxygen atoms of the support. The latter (nonbonding) contribution is represented by a shorter distance than that observed for the sample prepared from $[HRe(CO)_5]$ and titania treated at 573 K.

IR spectra demonstrate carbonate formation upon adsorption of $[CH_3Re(CO)_5]$ on titania: The IR spectra show that after $[CH_3Re(CO)_5]$ was adsorbed on any of the titania samples, peaks appeared at $\tilde{\nu}\approx1385$ and 1453 cm^{-1} (Figure 7), corresponding to adsorbed carbonate species (Table 5). The be-

havior is similar to what was observed when $[HRe(CO)_5]$ was adsorbed on our titania samples. Furthermore, the appearance of new peaks (not observed when $[HRe(CO)_5]$ was adsorbed) at $\tilde{\nu} \approx 1407$ and 1507 cm^{-1} was also observed for this sample.

Discussion

Effect of titania treatment conditions on Ti^{3+} site formation: consistency with the literature: In agreement with earlier reports,[9,18] our data show how the treatment conditions affect the titania surface-OH species. For example, when the titania was treated in flowing O_2, the bands associated with OH groups on Ti^{3+} sites were markedly reduced in intensity, relative to the same bands characterizing the titania that had been treated under vacuum (the reduction in band intensity is relative to the intensity of the band characteristic of the OH groups on Ti^{4+} sites).

The data also show that the number of Ti^{3+}–OH groups on titania relative to the total number of surface OH groups (determined by the relative peak areas) could be tuned by changing the temperature of the calcined titania during evacuation. When the evacuation temperature was increased, the intensity of the IR band associated with Ti^{3+}–OH groups ($\tilde{\nu} = 3717$ cm^{-1}) increased relative to the intensities of the bands associated with Ti^{4+}–OH and $(Ti^{4+})_2$–OH groups ($\tilde{\nu} = 3689$, 3672, and 3642 cm^{-1}).

IR spectra characterizing $TiO_{2vac723}$ and $TiO_{2vac573}$ after adsorption of $[CH_3Re(CO)_5]$ (1 wt% Re loading) show that although the amount of rhenium was the same, the spectrum characterizing $TiO_{2vac573}$ still indicated the presence of Ti^{3+}–OH, whereas the spectrum of $TiO_{2vac723}$ did not. Thus, we infer that there were more Ti^{3+}–OH sites on $TiO_{2vac573}$ than on $TiO_{2vac723}$ and, therefore, that the increase in treatment temperature led to the removal of Ti^{3+}–OH sites. Consequently, we infer that the increase in the number of Ti^{3+}–OH groups relative to Ti^{4+}–OH groups resulting from an increased treatment temperature shows that the OH groups on Ti^{3+} are more difficult to remove by heating than the OH groups on Ti^{4+} sites.

Decarbonylation of rhenium carbonyls and formation of surface carbonates and water: The EXAFS data characterizing $TiO_{2vac723}$ and TiO_{2ox723} after exposure to $[HRe(CO)_5]$ give no evidence of Re–Re contributions, indicating that the species formed during the adsorption were site-isolated rhenium complexes and not clusters. Moreover, the EXAFS data demonstrate the presence of supported rhenium species incorporating approximately three carbonyl groups per Re atom, indicating that decarbonylation of the rhenium as a result of the adsorption took place. Consistent with this inference, the IR spectra indicate rhenium tricarbonyls, as the ν_{CO} peaks were observed at positions matching those of rhenium tricarbonyls in solution[31,32] and on various metal oxide surfaces.[25,29,30]

Data characterizing the samples prepared from $[CH_3Re(CO)_5]$ show that this rhenium complex also was decarbonylated upon adsorption. However, the decarbonylation was less complete than that of $[HRe(CO)_5]$, as indicated by the EXAFS data, which demonstrate the presence of more carbonyl ligands per Re atom (approximately four) than on the supported rhenium made from $[HRe(CO)_5]$. This result was confirmed by the IR spectra, which suggest the presence of rhenium tetracarbonyls[42] (as well as other rhenium carbonyls).

The comparison of the surface species formed from $[HRe(CO)_5]$ and from $[CH_3Re(CO)_5]$ shows that these complexes have different reactivity towards titania—with $[HRe(CO)_5]$ being the more reactive in terms of the decarbonylation.

The decarbonylation of each of the rhenium complexes on titania was accompanied by the formation of surface species inferred to be carbonates and water. The possibility that carbonates were formed from the CH_3 groups of $[CH_3Re(CO)_5]$ is discounted, because carbonates were also formed from $[HRe(CO)_5]$. Thus, we infer that a source of carbon atoms in carbonates formed from $[HRe(CO)_5]$ were the carbonyl ligands on the rhenium, and the data do not rule out this possibility for $[CH_3Re(CO)_5]$ either.

Thus, we infer that a carbon atom and one of the oxygen atoms of each carbonate originated from the carbonyl groups on either $[HRe(CO)_5]$ or $[CH_3Re(CO)_5]$. We suggest that the other carbonate oxygen atoms originated from the titania surface, from at least one of the following sources: OH groups, oxygen radicals, and bridging oxygen groups on the titania surface. The participation of oxygen radicals cannot be probed with our methods and is not ruled out, but the results clearly demonstrate the removal of terminal OH groups from the titania surface when either of the rhenium complexes was adsorbed, and the concomitant formation of adsorbed water demonstrates that OH groups were a source of oxygen atoms in carbonate. Moreover, the presence of an isosbestic point in the spectra characterizing the sample during the adsorption of $[HRe(CO)_5]$ (Figure 6) is related to the decrease in the number of Ti^{3+}–OH and Ti^{4+}–OH groups and an increase in the number of $(Ti^{4+})_2$–OH groups and water molecules observed during the adsorption of $[HRe(CO)_5]$ and shows that the stoichiometry of the reaction of these groups was fixed—that they all participate in the same reaction.[43]

Thus, we hypothesize that the formation of carbonates on the titania involves the reaction of either of the rhenium carbonyls with terminal OH groups (removing these groups), leading to the release of hydrogen atoms that combine a) with titania OH groups (forming water) and/or b) with Ti^{4+}-O-Ti^{4+} groups (forming bridging hydroxyl groups).

Beyond this, we might speculate, on the basis of the results indicating the selective reaction of each of the rhenium complexes with terminal hydroxyl groups of titania, and in particular with OH groups associated with Ti^{3+} sites, that the surface species resulting from the adsorption of each of the rhenium complexes were bound at (or close to) the sites

initially containing Ti^{3+} atoms—thus, we would expect the latter sites to have been converted during the adsorption process, as was observed earlier[18] in samples in which $[H_3Re_3(CO)_{12}]$ was adsorbed on titania under vacuum.

Reactivity of titania with rhenium complexes: characterizing the relative reactivities of the various surface OH sites: IR spectra characterizing the OH region of $TiO_{2vac723}$ during the adsorption of $[HRe(CO)_5]$ show that the complex reacted selectively with the two kinds of terminal hydroxyl groups on the surface, Ti^{3+}–OH and Ti^{4+}–OH. Further evidence of the differences in reactivity of the two kinds of surface OH groups can be found in the results observed after adsorption of various amounts of $[CH_3Re(CO)_5]$ on $TiO_{2vac723}$. When a small amount of $[CH_3Re(CO)_5]$ was adsorbed (0.4 wt% Re), the Ti^{3+}–OH band decreased significantly in intensity, accompanied by an increase in intensity of the water peak. Addition of more $[CH_3Re(CO)_5]$ (1.0 wt% Re) led to almost complete removal of the Ti^{3+}–OH bands and significant reduction of one of the Ti^{4+}–OH bands ($\tilde{\nu}=$ 3689 cm^{-1}). Addition of still more $[CH_3Re(CO)_5]$ led to the complete removal of all terminal hydroxyl OH bands and a continued increase in the intensity of the water peak, which became very strong.

The pattern whereby the initial adsorption of $[CH_3Re(CO)_5]$ led to preferential removal of Ti^{3+}–OH groups but not Ti^{4+}–OH groups, whereas increased amounts of $[CH_3Re(CO)_5]$ adsorbed led increasingly to removal of Ti^{4+}–OH groups, leads us to propose that the reactivity of the surface hydroxyl groups with $[CH_3Re(CO)_5]$ is dependent on the O–H bond strength, which is related to the O–H stretching frequency—the OH groups with stronger O–H bonds (and weaker Ti–O bonds), react more readily with $[CH_3Re(CO)_5]$.[44]

Value of $[HRe(CO)_5]$ as a probe of oxide surface sites: The results presented here demonstrate the value of $[HRe(CO)_5]$ and $[CH_3Re(CO)_5]$ as probes of titania surface sites. We suggest that these compounds could be used similarly to characterize the reactivities of sites on other metal oxides as well, but we emphasize the need for handling of the oxide to ensure that the surface sites interact exclusively with the metal carbonyl and not with contaminants such as those present in air.

These probe molecules include metal atoms, and they provide information regarding the reactivities of the titania surface with metal complexes incorporating cationic species. In contrast to supported metal complexes, which are typically cationic,[2] the metal atoms in supported metal particles are usually essentially zero valent, at least when the metals are of groups 7 and 8.[45] However, when the metals, even group 8 metals, are present in clusters of only a few atoms on a metal-oxide support, the metal atoms at the metal–support interface may, with some generality, be cationic, as indicated by the metal–oxygen distances determined by EXAFS spectroscopy and by theoretical calculations at the level of density functional theory.[46] Thus, we might anticipate that the evidence of the metal–support interface determined in experiments such as ours might pertain to supported metals with some generality, especially when the metals are most highly dispersed.

In summary, families of organometallic complexes are well suited as probes of reactive metal-oxide surfaces because they are tunable and allow the variation of both the ligands and the metal in the probe. Specifically, the comparison of results obtained with our pair of probe molecules, $[HRe(CO)_5]$ and $[CH_3Re(CO)_5]$, provided information regarding the sources of carbon and hydrogen for the formation of the products observed in addition to the supported metal complexes. These products were surface carbonate species, bridging hydroxyl groups, and water. Thus, this pair of probe molecules provided substantially more insight into the surface chemistry than would have been obtained from the use of either of them alone.

Conclusion

The use of two rhenium complexes of the type $[LRe(CO)_5]$ (with L being CH_3^- and H^-) as probes of the titania surface, in conjunction with complementary spectroscopic methods, enabled the resolution of the effect of various treatment conditions on the concentrations of various surface OH groups. It also permitted us to gain insight into the reactivity of the surface OH groups, with the Ti^{3+}–OH sites being the more reactive with the probe molecules, but the less reactive in simple thermal dehydroxylation of the titania surface.

Identification of species formed and consumed during the adsorption of each of the two rhenium complexes provided insight into the chemistry of adsorption of the complexes on titania, information that would have been unavailable if only one of the complexes was used. Thus, the results demonstrate the value of using a family of similar probes as opposed to a single probe.

Experimental Section

Synthesis

Titania (anatase): Preparation of high-area porous anatase was carried out by the method of Wang et al.[47] The details are crucial, and so we present them here. A mixture of water (104 mL) and ethanol (50 mL, gold shield, 200 proof) was stirred for 5 min in a 600 mL beaker, and a solution of ethanol (50 mL) and titanium isopropoxide (10 g, Sigma–Aldrich, >97%) was added dropwise over a period of 5 min. The mixture was allowed to react for 2 h, and the resultant white solid was separated from the liquid by centrifugation and then washed by redispersing in ethanol (5×160 mL) and then centrifuging. The washed solid, a powder, was dried in a Petri dish at room temperature for a minimum of two days. For calcination, the dried powder was placed in a tubular quartz reactor and held in place by a quartz frit; the reactor was fitted with a thermocouple well extending to approximately 1 cm below the frit. The reactor was sealed with glass caps fitted with high-vacuum fittings and sealed with high-temperature vacuum grease (Apiezon H), and the solid was treated for 4 h at 723 K in flowing O_2 (Airgas, 99.8%).

To prepare titania incorporating a high density of surface Ti^{3+} sites, the calcination was immediately followed by a vacuum treatment at tempera-

tures in the range of 523–723 K.[18] After the treatment, the reactor was allowed to cool and, in the absence of air and moisture, the sample was transferred to an N_2-filled glovebox (the O_2 and H_2O concentrations were each <1 ppm) and stored until further use.

When a low density of surface Ti^{3+} sites was desired, the calcination was followed by a treatment in flowing O_2 at 723 K for 4 h.[18] Thereafter, the sample was cooled to a temperature <353 K, the reactor was evacuated for a minimum of 10 min and, in the absence of air and moisture, the sample was transferred to the glovebox until further use.

Rhenium carbonyl compounds

Caution: Metal carbonyls are extremely toxic. $[HRe(CO)_5]$ and $[CH_3Re(CO)_5]$ pose a high risk because of their relatively high vapor pressures. Any handling should be performed in a well-ventilated space and with appropriate protective equipment.

$[HRe(CO)_5]$: The synthesis of $[HRe(CO)_5]$ was carried out by the method of Urbancic and Shapley.[16] Tetraethylene glycol dimethyl ether (Sigma, 99%), phosphoric acid (EMD Science, 85%), phosphorus pentoxide (Sigma–Aldrich, 97%), zinc dust (Fisher, 99%), and rhenium carbonyl bromide (Strem, 98%) were used as received. All sample handling was done with the exclusion of air and moisture by the use of an N_2-filled glovebox, Schlenk techniques, and an argon-filled glovebag. In the final stage of the synthesis, the flask containing $[HRe(CO)_5]$ was exposed to air for a period of about 5 s as the flask was removed from the Schlenk line and capped. The $[HRe(CO)_5]$ was then purified by vacuum distillation through a bed of P_2O_5. The flask containing the $[HRe(CO)_5]$ was wrapped in aluminum foil (to avoid exposure to light) and stored at 273 K. The purity of the product in a solution of CH_2Cl_2 and in the gas phase was confirmed by IR spectroscopy.[41]

$[CH_3Re(CO)_5]$: The synthesis of $[CH_3Re(CO)_5]$ was carried out by a reported method.[17] Tetrahydrofuran (Acros Organics, 99.9%), $[Re_2(CO)_{10}]$ (Pressure Chemicals), mercury (Quicksilver Products), sodium (Sigma–Aldrich, 99%), and methyl iodide (Acros Organics, 99%) were used as received. The $[CH_3Re(CO)_5]$ was purified by vacuum distillation. Its identity was confirmed by IR spectroscopy.[17]

Adsorption of $[CH_3Re(CO)_5]$ and of $[HRe(CO)_5]$ on titania: The adsorption was carried out with strict exclusion of air and moisture by use of the inert-atmosphere gloveboxes and Schlenk techniques. The rhenium carbonyl in a sealed flask was briefly evacuated to remove any traces of moisture, and then it was placed in a cold bath (196 K for $[HRe(CO)_5]$ and 248 K for $[CH_3Re(CO)_5]$) and evacuated for a minimum of 20 min to remove any traces of O_2. The sealed flask was then placed in the glovebox and connected through a U-shaped glass tube fitted with a high-vacuum valve to a 15 mL two-neck flask containing the treated titania. The assembly contained the titania in one chamber and the rhenium carbonyl in the other (the sections were isolated from each other by a high-vacuum valve). The assembly was removed from the glovebox, and the section containing the rhenium carbonyl was placed in the cold bath so that the rhenium carbonyl vapor pressure was reduced. Next, the assembly was evacuated, and then, under static vacuum, the rhenium carbonyl was allowed to warm to room temperature and come in contact with the titania by transport through the gas phase. During this process, the titania powder was stirred with a magnetic stirrer. After 16 h of contact, the assembly was transferred to the glovebox, the section that initially contained the rhenium carbonyl was removed, and the solid sample was evacuated for at least 12 h.

The method described above pertains to both $[HRe(CO)_5]$ and $[CH_3Re(CO)_5]$ and their adsorption on titania. There were differences in detail, however, between the methods used for the two rhenium compounds, as summarized below: When $[CH_3Re(CO)_5]$ was used, this complex, a solid, was weighed in air and placed in a pear-shaped flask before the synthesis was carried out as described in the preceding paragraph. In contrast, when $[HRe(CO)_5]$ was used, its mass was not determined (because of its high volatility and toxicity). Instead, an excess of $[HRe(CO)_5]$ was allowed to come in contact with the titania, as described in the preceding paragraph.

Characterization by IR spectroscopy

IR spectra were collected with a Bruker 90v/s instrument equipped with an HgCdTe detector. The samples were scanned with a spectral resolution of 2 cm^{-1}; each spectrum reported here is the average of a minimum of 512 scans (total collection time was ca. 90 s).

When spectra were obtained with samples in the IR cell without gas flowing through it, the samples were in the form of wafers pressed between two KBr windows. These samples, in the glovebox, were mounted in a gas-tight cell (International Crystal Laboratories). The cell was removed from the glovebox and transferred to the spectrometer. Each sample was scanned under vacuum (the pressure was 1 mbar).

When spectra were obtained with samples in the presence of a flowing gas, each sample in the glovebox was pressed into a self-supporting wafer and placed in a gas-tight cell that was also a flow reactor (In-Situ Research Instruments); then the cell was transferred to the spectrometer without contacting of the sample with the atmosphere. Spectra were recorded as $[HRe(CO)_5]$ was being adsorbed on the anatase wafer. The rhenium carbonyl was brought in contact with the anatase sample in a stream of helium; the helium flowed over the $[HRe(CO)_5]$ in a pear-shaped flask, and the vaporized rhenium carbonyl was carried continuously to the IR cell, and spectra were recorded periodically.

In the initial stage of an experiment, the flask containing the metal carbonyl was placed in a cold bath (196 K for $[HRe(CO)_5]$) to minimize the amount of metal carbonyl in the gas phase. In the second stage of the experiment, the precursor was removed from the cold bath and allowed to warm to room temperature, so that the vapor pressure of the rhenium carbonyl compound increased and its partial pressure in the helium stream increased.

X-ray absorption spectroscopy

Data collection: X-ray absorption spectra were collected at beam line X-18B at the National Synchrotron Light Source (NSLS) at Brookhaven National Laboratory. The beam energy was selected by means of a Si-(111) double-crystal monochromator, with a minimum step size of 0.40 eV.

Approximately 0.08 g of each sample (the mass required for an absorbance of 2.5) in the glovebox was mixed with boron nitride (0.22 g, Sigma–Aldrich, 98%) and packed into a stainless-steel plate with a 26×8 mm^2 opening and then sealed with Kapton tape.

Each sample was scanned in transmission mode with gas-filled ion chambers used to measure the intensity of the X-rays entering and exiting the sample cell. A 13-element germanium detector was used to detect fluorescence from the sample; an energy window around the Re L_α lines was used to obtain the rhenium fluorescence. However, as a consequence of the position of the germanium K edge (11 103 eV), the data range of the EXAFS was limited to 12 k (where k is the photo-electron wave vector). Thus, the use of transmission data was preferred whenever possible. Furthermore, a hafnium reference foil was scanned simultaneously with the sample to allow calibration of the energy scale.

Extended X-ray absorption fine structure data analysis: Data reduction and analysis were performed with the aid of the software package XDAP.[48] First, at least four scans were aligned and then averaged to extend the range of data that could be analyzed. Analysis of the data was performed by using a "difference file" technique;[49] the functions used to construct the structural models and to minimize the error are shown elsewhere.[50] Fitting was done in k space and in R space (R is the interatomic distance) by using three k weightings (k^0, k^1, and k^2). In the fitting, the number of fitted parameters (4 per shell) did not exceed the number of statistically independent data points, as determined by the Nyquist theorem.[51]

The fit quality of each candidate model was evaluated by the value of $(\Delta\chi)^2$, as defined by the International XAFS Society.[33] Details of the analysis of the EXAFS data are essentially the same as those reported.[52] Details are presented in the Supporting Information, including criteria for selecting appropriate models, discrimination between models that provide good fits, and information about reference compounds.

Acknowledgements

This research was supported by the U.S. Department of Energy, Office of Energy Research, Basic Energy Sciences, Contract FG02-87ER15600. Portions of the work were carried out at the NSLS, which is supported by the U.S. Department of Energy, Office of Science, Basic Energy Sciences, under Contract No. DE-AC02-98CH10886. Beam line X18-B is supported by the NSLS, through the Divisions of Materials and Chemical Sciences of the DOE, and the Synchrotron Catalysis Consortium (DE-FG02-05ER15688). We thank the beam line staff for their assistance.

[1] L. Guczi, *Catal. Today* **2005**, *101*, 53.
[2] J. Guzman, B. C. Gates, *Dalton Trans.* **2003**, 3303.
[3] D. N. Belton, Y. M. Sun, J. M. White, *J. Am. Chem. Soc.* **1984**, *106*, 3059.
[4] E. J. Braunschweig, A. D. Logan, A. K. Datye, D. J. Smith, *J. Catal.* **1989**, *118*, 227.
[5] T. L. Thompson, J. T. Yates, *Top. Catal.* **2005**, *35*, 197.
[6] R. F. Howe, M. Grätzel, *J. Phys. Chem.* **1987**, *91*, 3906.
[7] Y. Nakaoka, Y. Nosaka, *J. Photochem. Photobiol. A* **1997**, *110*, 299.
[8] M. Arai, S. Guo, Y. Nishiyama, *Appl. Catal.* **1991**, *77*, 141.
[9] S. H. Szczepankiewicz, A. J. Colussi, M. R. Hoffman, *J. Phys. Chem. A* **2000**, *104*, 9842.
[10] K. Hadjiivanov, H. Knözinger, *Surf. Sci.* **2009**, *603*, 1629.
[11] T. L. Thompson, O. Diwald, J. T. Yates, *J. Phys. Chem. B* **2003**, *107*, 11700.
[12] J. C. Lavalley, *Catal. Today* **1996**, *27*, 377.
[13] S. Huber, H. Knözinger, *Chem. Phys. Lett.* **1995**, *244*, 111.
[14] Del Vitto, L. Giordano, G. Pacchioni, N. Rösch, *Surf. Sci.* **2005**, *575*, 103.
[15] D. F. Shriver, P. W. Atkins, *Inorganic Chemistry*, 3rd ed., Oxford University Press, New York, **1999**.
[16] M. A Urbancic, J. R. Shapley, *Inorg. Synth.* **1989**, *26*,77.
[17] C. E. Zybill in *Transition Metals, Synthetic Methods of Organometallic and Inorganic Chemistry, Vol. 7, Part 1* (Ed.: W. A. Herrmann), Thieme, New York, **1997**, pp. 97–98.
[18] K. Suriye, R. J. Lobo-Lapidus, G. Y. Yeagle, R. D. Britt, B. C. Gates, *Chem. Eur. J.* **2008**, *14*, 1402.
[19] S. Vuk, R. Jese, M. Gaberscek, B. Orel, G. Drazic, *Sol. Energy Mater. Sol. Cells* **2006**, *90*, 452.
[20] Morterra, *J. Chem. Soc. Faraday Trans.* **1988**, *84*, 1617.
[21] K. I. Hadjiivanov, D. G. Klissurski, *Chem. Soc. Rev.* **1996**, *25*, 61.
[22] The Ti^{3+}–OH group is expected to have the highest OH stretching frequency of all the OH groups on the titania, because the partially reduced Ti^{3+} is expected to be more weakly bonded to the OH group than the others, which would produce stronger O–H bonds and, thus, higher vibrational frequencies.
[23] M. A. El-Sayed, H. D. Kaesz, *J. Mol. Spectrosc.* **1962**, *9*, 310.
[24] J. B. Wilford, F. G. A. Stone, *J. Organomet. Chem.* **1964**, *2*, 371.
[25] P. S. Kirlin, F. B. M. van Zon, D. C. Koningsberger, B. C. Gates, *J. Phys. Chem.* **1990**, *94*, 8439.
[26] J. Dalton, I. Paul, F. G. A. Stone, *J. Chem. Soc. A* **1968**, 1212.
[27] J. A. M. Andersen, J. R. Moss, *J. Organomet. Chem.* **1995**, *494*, 105.
[28] K. Edgar, J. Lewis, A. R. Manning, J. R. Miller, *J. Chem. Soc. A* **1968**, 1217.
[29] P. S. Kirlin, F. A. DeThomas, J. W. Bailey, H. S. Gold, C. Dybowski, B. C. Gates, *J. Phys. Chem.* **1986**, *90*, 4882.
[30] H. M. Sung-Suh, D. S. Kim, C. W. Lee, S. Park, *Appl. Organomet. Chem.* **2000**, *14*, 826.
[31] F. Zobi, O. Blacque, H. W. Schmalle, B. Spingler, R. Alberto, *Inorg. Chem.* **2004**, *43*, 2087.
[32] U. Sartorelli, F. Canziani, F. Zingales, *Inorg. Chem.* **1966**, *5*, 2233.
[33] International XAFS Society, Error Reporting Recommendations: A Report of the Standards and Criteria Committee, http://www.i-x-s.org/OLD/subcommittee_reports/sc/err-rep.pdf (accessed September 2009).
[34] S. Fung, P. A. Tooley, M. J. Kelley, D. C. Koningsberger, B. C. Gates, *J. Phys. Chem.* **1991**, *95*, 225.
[35] R. J. Lobo-Lapidus, M. J. McCall, M. Lanuza, S. Tonnesen, S. R. Bare, B. C. Gates, *J. Phys. Chem. C* **2008**, *112*, 3383.
[36] L.-F. Liao, C. F. Lien, D. L. Shieh, M.–T. Chen, J.–L. Lin, *J. Phys. Chem. B* **2002**, *106*, 11240.
[37] D. J. C. Yates, *J. Phys. Chem.* **1961**, *65*, 746.
[38] Y. Hao, M. Mihaylov, E. Ivanova, K. Hadjiivanov, H. Knözinger, B. C. Gates, *J. Catal.* **2009**, *261*, 137.
[39] W. Su, J. Zhang, Z. Feng, T. Chen, P. Ying, C. Li, *J. Phys. Chem. C* **2008**, *112*, 7710.
[40] F. A. Miller, C. H. Wilkins, *Anal. Chem.* **1952**, *24*, 1253.
[41] P. S. Braterman, R. W. Harrill, H. D. Kaesz, *J. Am. Chem. Soc.* **1967**, *89*, 2851.
[42] E. Leins, N. J. Coville, *J. Organomet. Chem.* **1991**, *407*, 359.
[43] *IUPAC, Compendium of Chemical Terminology*, 2nd ed. (Eds.: A. D. McNaught, A. Wilkinson), Blackwell Scientific Publications, Oxford, **1997**). XML on-line corrected version: http://goldbook.iupac.org created by M. Nic, J. Jirat, B. Kosata; updates compiled by A. Jenkins. (accessed September 2009).
[44] This trend in the reactivity of the surface OH groups with rhenium carbonyls to form rhenium tricarbonyls is contrasted with the reactivity of these OH groups with other OH surface groups to form water during high-temperature treatment, whereby the OH groups in Ti^{3+}–OH groups appear to be less reactive than those in Ti^{4+}–OH groups.
[45] M. Boudart, *J. Mol. Catal.* **1985**, *30*,27.
[46] G. N. Vayssilov, B. C. Gates, N. Rösch, *Angew. Chem.* **2003**, *115*, 1429; *Angew. Chem. Int. Ed.* **2003**, *42*, 1391.
[47] C. C. Wang, J. Y. Ying, *Chem. Mater.* **1999**, *11*, 3113.
[48] M. Vaarkamp, J. C. Linders, D. C. Koningsberger, *Physica B+C* **1995**, *209*, 159.
[49] J. B. A. D. van Zon, D. C. Koningsberger, H. F. J. van't Blik, D. E. Sayers, *J. Chem. Phys.* **1985**, *82*, 5742.
[50] D. C. Koningsberger, B. L. Mojet, G. E. van Dorssen, D. E. Ramaker, *Top. Catal.* **2000**, *10*, 143.
[51] E. A. Stern, *Phys. Rev. B* **1993**, *48*, 9825.
[52] V. Aguilar-Guerrero, R. J. Lobo-Lapidus, B. C. Gates, *J. Phys. Chem. C* **2009**, *113*, 3259.
[53] B. Enderle, B. C. Gates, *Phys. Chem. Chem. Phys.* **2004**, *6*, 2484.

Received: January 31, 2010
Published online: August 19, 2010

